25. S. Grebenev *et al.*, *J. Chem. Phys.* **112**, 4485 (2000).
26. K. Nauta, R. E. Miller, *Phys. Rev. Lett.* **82**, 4480 (1999).
27. P. L. Stiles, D. T. Moore, K. Nauta, R. E. Miller, in preparation.
28. M. Hartmann, R. E. Miller, J. P. Toennies, A. F. Vilesov, *Phys. Rev. Lett.* **75**, 1566 (1995).
29. C. Callegari *et al.*, *Phys. Rev. Lett.* **83**, 5058 (1999).
30. Y. Kwon, P. Huang, M. V. Patel, D. Blume, K. B. Whaley, *J. Chem. Phys.* **113**, 6469 (2000).
31. K. Nauta, thesis, University of North Carolina at Chapel Hill (2000).
32. D. V. Lanzisera, L. Andrews, *J. Phys. Chem. A* **101**, 9666 (1997).
33. Points on the potential energy surface were calculated [MP2/6-311++G(2df,2pd)] with the Mg atoms fixed in the equilibrium trimer geometry (*24*). The distance of the HCN from the Mg_3 plane was varied, as was the angle made by the HCN with the Mg_3 plane.
34. K. Nauta, R. E. Miller, in preparation.
35. The N-Mg distances for HCN-Mg and HCN-Mg_2 are taken from MP2/6-311++G(3df,3pd) geometry optimizations, whereas the distance for HCN-Mg_3 is interpolated from the PES scan described in (*34*).
36. O. C. Thomas, W. Zheng, K. H. Bowen, private communication.
37. J. M. Sin, S. Nayak, G. Scoles, in *Cluster and Nanostructure Interfaces*, P. Jena, S. N. Khanna, B. K. Rao, Eds. (World Scientific, Singapore, 2000), pp. 345–352.
38. This work was supported by the NSF (CHE-99-87740). We also acknowledge the donors of the Petroleum Research Fund, administered by the American Chemical Society, and the Air Force Office for Scientific Research (AFOSR) for partial support of this research. We thank G. Scoles for helpful discussions during the preparation of this manuscript and K. H. Bowen for permitting us to quote his results as a private communication.

11 January 2001; accepted 6 March 2001

Imaging of Small-Scale Features on 433 Eros from NEAR: Evidence for a Complex Regolith

J. Veverka,[1] P. C. Thomas,[1] M. Robinson,[2] S. Murchie,[3] C. Chapman,[4] M. Bell,[1] A. Harch,[1] W. J. Merline,[4] J. F. Bell III,[1] B. Bussey,[2] B. Carcich,[1] A. Cheng,[3] B. Clark,[1] D. Domingue,[3] D. Dunham,[3] R. Farquhar,[3] M. J. Gaffey,[5] E. Hawkins,[3] N. Izenberg,[3] J. Joseph,[1] R. Kirk,[6] H. Li,[2] P. Lucey,[7] M. Malin,[8] L. McFadden,[9] J. K. Miller,[10] W. M. Owen Jr.,[10] C. Peterson,[1] L. Prockter,[3] J. Warren,[3] D. Wellnitz,[9] B. G. Williams,[10] D. K. Yeomans[10]

On 25 October 2000, the Near Earth Asteroid Rendevous (NEAR)–Shoemaker spacecraft executed a low-altitude flyover of asteroid 433 Eros, making it possible to image the surface at a resolution of about 1 meter per pixel. The images reveal an evolved surface distinguished by an abundance of ejecta blocks, a dearth of small craters, and smooth material infilling some topographic lows. The subdued appearance of craters of different diameters and the variety of blocks and different degrees of their burial suggest that ejecta from several impact events blanketed the region imaged at closest approach and led to the building up of a substantial and complex regolith consisting of fine materials and abundant meter-sized blocks.

Data obtained during the early phases of NEAR's orbital mission answered many first-order questions about the global and regional characteristics of asteroid 433 Eros (*1*). These data confirmed that the surface is covered with regolith (*2*) and contained hints that the regolith is complex. To better understand the processes that have shaped the surface of Eros and determined the characteristics of its regolith, higher resolution images were needed.

On 25 October 2000, the NEAR spacecraft executed a low-altitude flyover (LAF), during which it swept down to 6.4 km above the surface of Eros, permitting the multispectral imager (MSI) camera to view the surface at a resolution of 1 m per pixel, which is about four times better than the best previous views. About 250 images were obtained during the LAF through the camera's 950-nm filter, in addition to two isolated three-color spot views using the 550-, 760-, and 950-nm filters (*3*). A narrow belt of coverage was obtained around Eros at mid-southern latitudes at altitudes below 30 km (resolution ≤4 m). Images obtained at altitudes below 10 km covered a thin strip between 34°S, 359°W to 4°S, 45°W. Closest approach (19.9°S, 27.8°W) occurred at an altitude of 6.43 km (with a resolution of about 1 m per pixel). The solar phase angle at closest approach was 97° (*4*). The only comparable data for airless bodies are images of the moon and the Mars satellite Phobos (*5*).

Our images reveal a complex surface marked by diverse evidence of regolith, a dearth of small impact craters, and an abundance of positive relief features (PRFs), most likely ejecta blocks (Fig. 1). The high-resolution images cover cratered terrains on Eros and do not cross into the two major depressions on the asteroid: the 9.4-km saddle Himeros and the 5.2-km crater Psyche (*1*). The images show a subdued, gently undulating surface characterized by abundant blocks and conspicuously degraded craters. Many of the degraded craters show evidence of infilling. A novel feature is the occurrence of smooth flat areas (hereafter referred to as ponds) in the interiors of certain craters (Fig. 2), features that to our knowledge have not been noted before in images of Phobos or of Deimos (*5*). No other asteroid has been imaged at comparable resolution. The region of high-resolution coverage is crossed in a few places by linear depressions ("grooves"), which can be traced out in previous lower resolution images.

Color observations obtained during the LAF show no difference between the colors of blocks and those of the surrounding regolith. Lower resolution images had shown albedo and color differences associated with steep slopes in certain regions, especially within the crater Psyche and the saddle Himeros (*6*). Two sets of three-color images at 550, 760, and 950 nm were acquired during the low-altitude flyover (*7*). One of the areas contains a large number of boulders and several smooth pond deposits. Most boulders in the size range of 5 to 10 m show no color difference from the background regolith, a finding consistent with results for larger boulders (~50 m) from earlier data obtained during the 50-km orbit (*6*). The ponds, on average, have a slightly higher 560/760-nm ratio (0.69 versus 0.67) and a slightly lower 950/760-nm ratio (0.94 versus 0.95), but the difference is very small and may not be signif-

[1]Space Sciences Building, Cornell University, Ithaca, NY 14853, USA. [2]Department of Geological Sciences, Northwestern University, 309 Locy Hall, Evanston, IL 60208, USA. [3]Applied Physics Laboratory, Johns Hopkins University, 1110 Johns Hopkins Road, Laurel, MD 20723, USA. [4]Southwest Research Institute, 1050 Walnut Street, Suite 426, Boulder, CO 80302, USA. [5]Department of Earth and Environmental Sciences, Science Center, Rensselaer Polytechnic Institute, 110 8th Street, Troy, NY 12180–3590, USA. [6]U.S. Geological Survey, 2255 North Gemini Drive, Flagstaff, AZ 86001, USA. [7]Hawaii Institute of Geophysics and Planetology, University of Hawaii, 2525 Correa Road, Honolulu, HI 96822, USA. [8]Malin Space Science Systems, Post Office Box 910148, San Diego, CA 92191, USA. [9]Department of Astronomy, University of Maryland, College Park, MD 20742, USA. [10]Jet Propulsion Laboratory, 4800 Oak Grove Drive, Pasadena, CA 91109, USA.

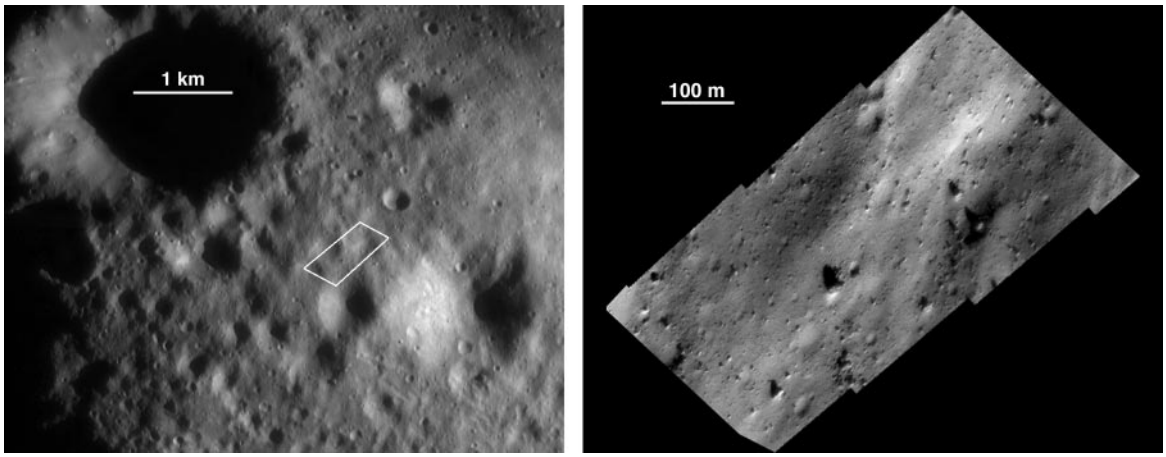

Fig. 1. Typical segment of LAF coverage (right) centered at (24.1°S, 19.2°W). The region (left) is located in the vicinity of crater Selene (which is about 3 km in diameter) and is representative of the cratered terrains on Eros. The closeup view at right is a mosaic of four frames at mission elapsed time (MET) 147953203 to 147953253 s and has a scale of about 1.2 m per pixel. The context view at left is a mosaic of frames at MET 145906548 to 145906743 s.

icant because of our very limited sample. We conclude that on average, the boulders, and probably the ponds, share the color properties of the background. One explanation of the homogeneous color properties observed to the smallest scales is that this entire region is covered with at least an optically thick (tens of microns or more) homogeneous layer of fine dust.

The high-resolution images are dominated by an abundance of PRFs, which are interpreted as ejecta blocks derived from cratering events on Eros. The abundance of presumed ejecta blocks was already noted (*1*) on the basis of medium-resolution images (~20 m per pixel). The LAF images show that blocks down to a meter in size are a dominant feature of the Eros landscape. The LAF coverage includes two blocks over 50 m across (but less than 15 m high) near the edge of Shoemaker Regio (20°S, 330°W), an area of very abundant blocks (*1*). The number of blocks increases rapidly as the diameter of the blocks decreases. The size distribution of blocks is described adequately by a power law with a slope of about –3 on a cumulative plot. At scales of 3 to 5 m, there are about 100 times more blocks than there are impact craters (Fig. 3).

The areal density of blocks is non-uniform in the high-resolution coverage; the primary concentrations occur in association with the crater Psyche (5.2 km across) and with the depression Shoemaker Regio (7 km across). The maximum density of blocks greater than 8 m in diameter observed in the LAF coverage is 99 per square kilometer; the least is about 6 per square kilometer. We estimate that there are on average about 25 blocks larger than 8 m across per square kilometer in this region of Eros and probably 500 times as many blocks larger than 1 m across. Craters larger than about 150 m in diameter are expected to produce blocks as large as 8 m (*8*).

The blocks display a wide range of morphologies and of apparent depths of burial.

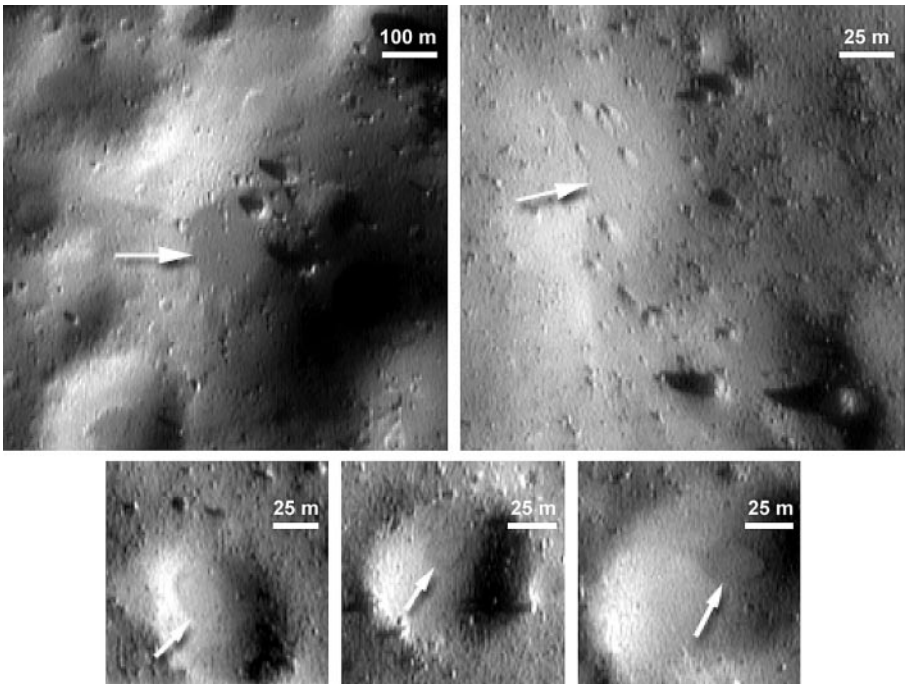

Fig. 2. Examples of flat-floored sediment ponds. Most often (bottom row) such features are found on crater floors, offset from the crater center toward the downslope side. Similar flat floor areas occur in noncrater depressions on Eros (top row). The flatness of the deposits suggests that fine-grained materials are involved. Because of regional slopes, the gravitationally lowest point within a small crater need not coincide with the center of the crater interior. Images used are at MET 147932871 s (top left), 147933203 s (top right), 147933303 s (bottom left), and 147934153 s (bottom center and right).

Our data suggest that the presumed ejecta blocks have a variety of mechanical competence. Some blocks display a marked angular, and in a few cases slablike, appearance suggestive of competent material. Others are much more rounded and even clumplike, shapes that are consistent with weaker materials. There is no strong correlation between block morphology and size. Occasionally, blocks appear to cluster on the surface (Fig. 1, bottom). Some blocks cluster near the rims of craters, and there may be alignments of ejecta blocks, but the high-resolution coverage is too restricted to support statistical tests of this suggestion. There is also a wide range of apparent degree of burial of the blocks. Although some of the most conspicuous blocks seem to be perched on the surface, others are buried to various degrees in a finer regolith. If one assumes that on average ejecta blocks are equidimensional, then the ratio of observed width to height (measured from shadows) gives a measure of burial depth. Typically, for blocks having widths in the range of 8 to 30 m, measured heights are about 0.7 of the width, suggesting depths of

burial from 2.5 to 10 m. Smaller blocks may be buried relatively more deeply than larger blocks, judging from somewhat smaller height/width ratios measured for the smaller blocks, which suggests that this region was covered with several meters of ejecta in a late event that affected the area. It is not known whether the underlying surface is consolidated or not.

Some of the block clusters may indicate the breakup of a clump of ejecta on impact with the surface. However, no secondary pits or gouges have been noted nor has evidence been found of boulders rolling on the surface, though these phenomena are also rare or absent on Phobos and Deimos (*5*). A few of the larger blocks are surrounded by debris aprons, suggesting that some erosion or disintegration occurred during or after emplacement. The example shown in Fig. 4 indicates that erosion of relatively fine material from the boulder occurred after the formation of the flat sedimentary fill on the crater floor and that the material eroded by impacts or possibly by thermal fracturing was separated from the block at low velocity (*9*).

Although there is abundant evidence of regolith features, evidence of "bedrock" exposures remains elusive, though it cannot be ruled out everywhere on Eros. Although the surface nearly ubiquitously displays blocks, filling of craters, groove forms, slumps, talus, and smooth deposits, no clear mechanical contrast of surface materials with deeper sections is suggested by crater morphologies. In all of the NEAR images, none of the craters shows the concentric or flat-floored morphology indicative of excavation through mechanical discontinuities that has been observed on the moon and on Phobos (*5*, *10*). This evidence for gradational changes of properties with depth may indicate that only poorly defined boundaries exist between surficial loose material and deeper materials. Additionally, no clear outcrops of distinct materials are seen in the LAF or other images; only rare, approximate alignments of blocks are seen that do not resemble outcrops and that occur in settings indicative of blocks resting on other units. The fine textures (at ~2 to 3 m scale) suggested in many of the LAF images, at the practical limit of resolution, are consistent with forms on loose materials, especially if reflecting large numbers of very small blocks or clumps.

We interpret the blocks as ejecta from impact events on Eros. Blocks in the size range of 10 to 30 m are expected to be produced copiously during the formation of craters 200 m to 1 km in diameter or larger (*8*). The variety of blocks and of their degree of burial suggest that the surface is the result of multiple events that deposited ejecta into this region and led to the buildup of a heterogeneous regolith consisting of fine materials and abundant sizeable blocks.

The abundance of ejecta blocks on Eros might be explained in at least two ways. First, it is possible that blocky ejecta from impacts may be formed more readily on a small body because less work is required to excavate fragmented materials. Almost certainly, such blocky ejecta will be dispersed more widely than on a larger body. Second, it is possible that because of its extended collisional history, Eros may be an inherently fractured body (*11*).

Craters as small as about 20 m in diameter can be studied in detail in the LAF area, and they display a broad range of morphologies reflecting a spectrum of degradation states (Fig. 5). Most craters are subdued and display evidence of infilling. A few craters display prominent shadows in their interiors and allow measurement of the depth-to-diameter ratio. A consistent maximum depth (d) to diameter (D) ratio of $d/D \sim 0.2$ is found for such craters over the diameter range of 20 to 100 m; this ratio is

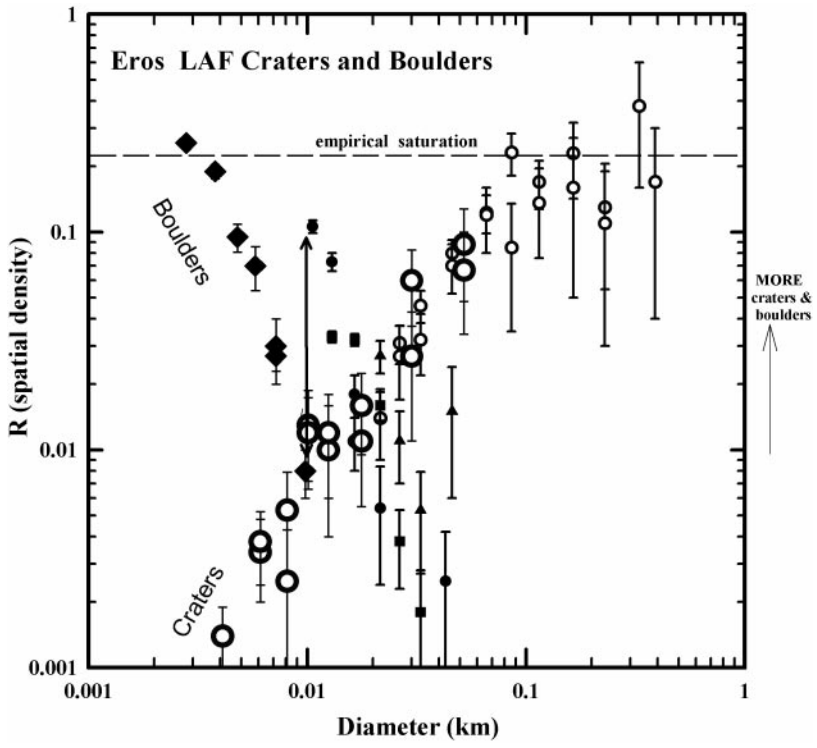

Fig. 3. Abundance of craters and boulders as a function of diameter D in the LAF region. This log-log R plot shows the numbers of craters and boulders on selected regions of Eros as a function of D. Differential frequencies (craters or boulders per square kilometer per kilometer increment of diameter) are divided by D^{-3}, so that spatial density increases upward toward saturated densities, shown approximately by the horizontal dashed line; saturated craters on the lunar maria approximately follow this line for diameters smaller than a few hundred meters. Data from the LAF images are shown by the larger symbols; the smaller symbols show counts from earlier high-resolution images taken during orbits at an altitude of 35 km. Open circles are craters; solid noncircular symbols (different shapes indicate different localities on Eros) are boulders and other PRFs. The densities of boulders and PRFs vary appreciably. Error bars reflect only counting statistics.

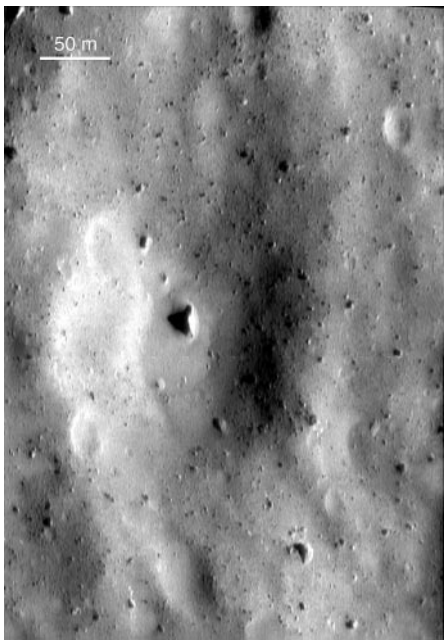

Fig. 4. Large block with debris apron. The prominent angular block (25 m long) sits on the floor of a shallow degraded crater 175 m in diameter. A debris apron extends about 5 m from the base of the block. There is an extensive flat area of sedimentary fill in this crater, similar to the sediment ponds shown in Fig. 2. This is a two-frame mosaic at MET 14953453 and 14953478 s. The block is at 20.35°, 27.3°W.

identical to that found for fresh craters on the moon (*12*) and is comparable with values found for other asteroids (*1*).

Crater counts reveal a paucity of small craters as compared to expected extrapolations from larger crater sizes or from what is observed on the moon (*13*). Although the surface of Eros is observed to be close to the empirical saturation limit for craters in the diameter range of 500 to 1000 m (Fig. 3), the surface density of craters 30 m in diameter is a factor of 10 below this limit; for craters 3.5 m in diameter, the depletion exceeds a factor of about 100. There are about 200 craters larger than 3.5 m in diameter per square kilometer in the LAF area. On Phobos, in the vicinity of the large crater Stickney, the density of craters 30 m in diameter is only slightly higher than on Eros (*5*).

It is difficult to explain the scarcity of small craters on Eros. There are sufficient projectiles in near-Earth space to produce small craters. Therefore, there must be a process that covers or erodes small craters on Eros much more effectively than is the case on the moon, or else we are seeing Eros soon after an impact event that deposited ejecta over the LAF region. One degradational process that ought to be much more efficient on a small body such as Eros as compared to the moon is seismic shaking of the surface after impacts (*14*).

A single blanketing event by ejecta would destroy all craters smaller than a threshold size in an area, preserve somewhat larger craters in a degraded state, and have a minimal effect on the largest craters. The gradual depletion of craters with diameters smaller than 100 m argues for a continuous process of degradation and erasure. In addition to blanketing by ejecta from a series of impact events and possibly the effects of associated seismic shaking, other degradation processes such as microcratering and thermal creep could play a role (*9*).

On Eros, distinctive flat floors are seen in many craters less than 300 m in diameter (Fig. 2). These features do not resemble flat-floored or bench craters on the moon or Phobos (*5*) that have been interpreted as the result of impact on a regolith underlain by a harder substrate. Larger, flat-floored craters on the moon have in some instances been attributed to seismically induced mass wasting (*14*); these have floors that appear less smooth than the Eros ponded materials. On Eros, smooth flat floors tend to occur in craters that appear morphologically substantially degraded; if they were exposures of a harder substrate, they would be most common in the least degraded craters.

The accumulations of ponded materials are sometimes offset from the center of the crater in which they occur. In areas with well-determined regional slopes, the flat floor areas occur preferentially on the downslope side of the crater, suggesting that regolith movement is implicated. However, the craters with flat floors do not show any noticeable morphology or albedo evidence of downslope movement on the crater walls, and the boundaries between the flat floors and crater walls are often very sharp. No significant color differences between the flat floor materials and the crater walls have been detected. No analogous features have been identified in comparable images of Phobos.

A characteristic of the flat floor ponds is that they typically occupy about one-third of the diameter of the parent crater in craters ranging from 20 to 300 m. Assuming a likely shape for fresh craters, a simple calculation indicates that craters in this size range have depths of ponded materials equal to about 5% of the crater diameter (*15*). Thus, the depth of material represented by such ponds is relatively small and non-uniform, ranging from about 1 m for a 20-m crater to about 5 m for a 100-m crater. The actual amounts may be much less because the craters were probably degraded by a combination of impact erosion and ejecta blanketing before the flat-floor fill was emplaced. The observation that craters in the same area have different depths of ponded material and that this depth is a definite function of crater size rules out the hypothesis that these ponds represent concentrations of a uniform widespread ejecta cover from one or

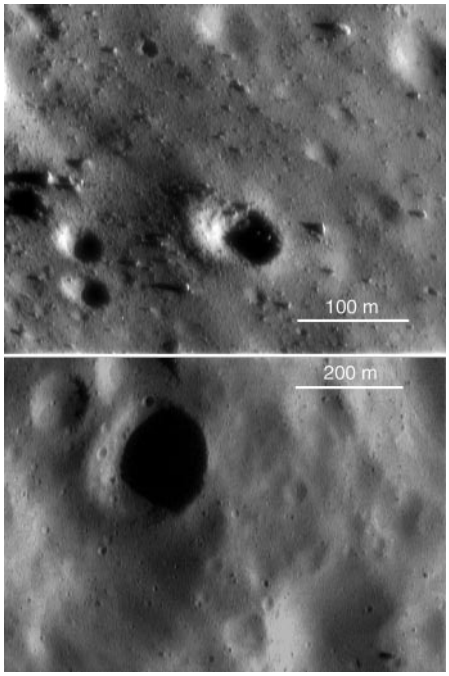

Fig. 5. Range of crater morphologies. Measurements show that the craters with prominent shadows have *d*/*D* ratios of about 0.2, a value similar to that of fresh lunar craters. Most craters, however, are very shallow and display a degraded appearance. At top is a region at 26.7°S, 13.7°W (MET 147953078 s). At bottom is a region at 58.2°S, 14.3°W (MET 147949633 s).

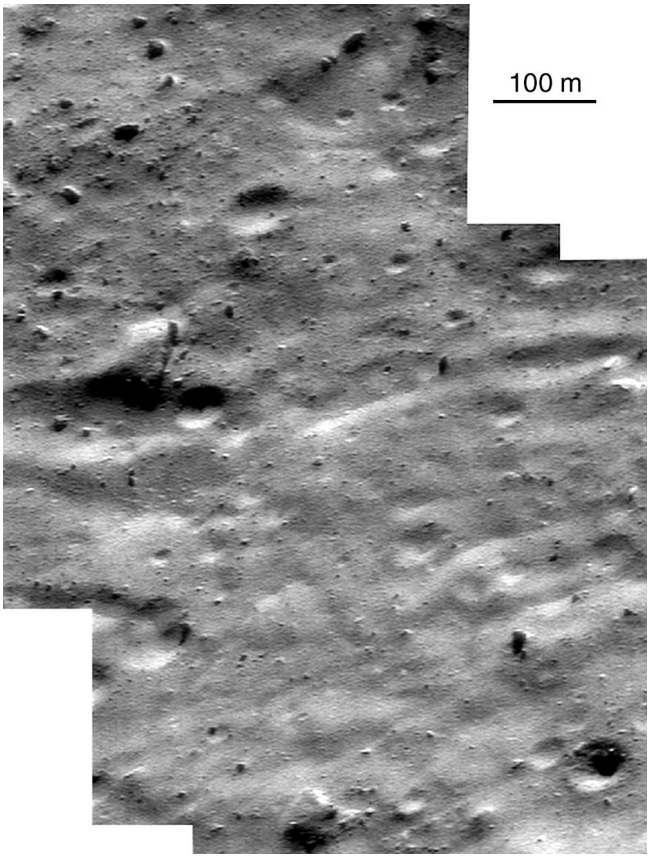

Fig. 6. Region near 52°S, 332°W crossed by groove-like linear troughs. Also prominent in this view are two very large (50-m) blocks. This is a mosaic from frames MET 147952-013 to 147952069 s.

more cratering events. It is perhaps significant that morphologically similar smooth, flat-floored areas of presumably ponded materials are seen in some other (noncrater) depressions on Eros (Fig. 2). Evidently there is an effective process on Eros that separates fine-grained materials from coarser regolith. Either this same process or another mechanism is able to transport the fine-grained materials over considerable lateral distances (*16*).

Some linear features, mostly grooves, previously identified in lower resolution images, can be found in the high-resolution LAF coverage as elongated depressions some tens of meters in width (Fig. 6). They are subtle depressions up to 25 m in depth (measured from shadows) with varying widths and amounts of asymmetry in profiles. Many have v-shaped cross sections indicative of the collapse of loose materials. Although some have superposed craters, indicating considerable age, other sections have sharp slope intersections and well-defined crests that may be younger. As with grooves on other bodies (*17*), their ultimate origin may be related to fractures in a more solid interior, but their surface expressions are controlled by the properties of loose materials, which may have been disturbed and in effect partially refreshed, multiple times while some other crater-induced degradation has occurred.

The LAF images provide evidence that Eros has a widespread regolith, typically several tens of meters in thickness. Exceptions may occur, especially locally on steep slopes (*18*). Similar indications of thick regoliths on small bodies have been deduced from spacecraft investigations of the tiny moons of Mars, Phobos and Deimos (*5*), and of asteroids 243 Ida (*19*) and 253 Mathilde (*20*).

References and Notes

1. For general characteristics of Eros, see J. Veverka *et al.*, *Science* **289**, 1993 (2000).
2. "Regolith" is used here in the general sense of unconsolidated fragmental material, regardless of formation or transport mechanisms.
3. The NEAR camera, the MSI, covers the spectral range from 400 to 1000 nm and has a 2.25°-by-2.90° field of view. The 244-by-537–pixel Thomson charge-coupled device has rectangular pixels that subtend 9.5 m by 16.1 m at 100 km. For details, see S. E. Hawkins *et al.*, *Space Sci. Rev*. **82**, 31 (1997) and J. Veverka *et al.*, *J. Geophys. Res*. **102**, 23709 (1997).
4. The solar incidence angle was 59° and the viewing (or emission) angle was 39°.
5. For Phobos, see P. C. Thomas *et al.*, *J. Geophys. Res*. **105**, 15,091 (2000). For the moon, see P. H. Schultz, *Moon Morphology* (Univ. of Texas Press, Austin, TX, 1976). Deimos, the outer satellite of Mars, was viewed by Viking at a resolution of 3 to 4 m [see P. C. Thomas, J. Veverka, *Icarus* **42**, 234 (1980)].
6. S. Murchie *et al.*, *Icarus*, in press.
7. For detailed passbands of filters and for reduction procedures used in analyzing MSI color data, see S. Murchie *et al.*, *Icarus* **140**, 66 (1999).
8. This calculation was done using the scaling given by P. Lee *et al.*, *Icarus* **120**, 87 (1996). If L is the size in meters of the largest block produced during the excavation of a crater of diameter D (in meters), then $L \sim 0.25\ D^{0.7}$. The largest blocks in the LAF area are about 60 to 70 m across, corresponding to a crater 3 km in diameter or larger (that is, the size of Selene or bigger).
9. For a good discussion of various possible erosional and degradational processes on airless bodies, see J. F. Lindsay, *Lunar Stratigraphy and Sedimentology* (Elsevier Scientific, New York, 1976).
10. W. L. Quaide, V. R. Oberbeck, *J. Geophys. Res*. **73** 5247 (1968).
11. Mars crossers such as Eros are in unstable orbits and must have spent most of the time since their formation in the main asteroid belt where collisions could have been relatively frequent during the earliest epochs [see P. Michel *et al.*, *Astron. J*. **116**, 2023 (1998)].
12. R. J. Pike, in *Impact and Explosion Cratering*, D. J. Roddy, R. O. Pepin, R. B. Merill, Eds. (Pergamon, New York, 1977), p. 489–509.
13. G. B. Neukum *et al.*, *Moon* **12**, 201 (1975).
14. P. H. Schultz, D. E. Gault, *Proc. Lunar Sci. Conf*. **6**, 2862 (1975).
15. The amount of material can be estimated by assuming a crater profile somewhat reduced from a fresh crater parabolic form with a depth/diameter (d/D) ratio of 0.2 (*12*). For a crater depth of 0.15 D, a central one-third of the crater would have a maximum depth of one-ninth the rim depth, or 0.017 D. For a linear depth/radius model, the deposit thickness would be one-third of the crater depth, or 0.05 D. These end-member estimates give a maximum depth of fill in a 100-m crater of 1.7 to 5 m, and a depth of fill of less than 1 m for a 20-m crater. It cannot be argued that the observed relationship between pond depth and crater diameter is explained because larger craters are on average older (form less frequently) than smaller craters and thus have had more time to accumulate ejecta from successive impact events. In such a case, at least some of the smaller craters would be expected to have as much fill as the larger ones, something that is not observed.
16. It has been suggested that electrostatic effects can both levitate and transport fine dust on airless bodies such as asteroids and the moon [see P. Lee, *Icarus*, **124**, 181 (1996) and T. Gold, *Mon. Not. R. Astron. Soc*. **115**, 585 (1955)].
17. J. Veverka *et al.*, *Icarus* **107**, 72 (1994); P. C. Thomas, J. Veverka, *Icarus* **40**, 394 (1979).
18. M. T. Zuber *et al.*, *Science* **289**, 2097; A. F. Cheng *et al.*, *Icarus*, in press.
19. R. Sullivan *et al.*, *Icarus* **120**, 119 (1996).
20. J. Veverka *et al.*, *Science* **285**, 562 (1999).

21. We thank the Mission Design, Mission Operations, and Spacecraft teams of the NEAR Project at the Applied Physics Laboratory of Johns Hopkins University for their dedicated and successful efforts that resulted in achieving the closest ever flyover of a solar system body by an orbiting spacecraft.

27 December 2000; accepted 7 March 2001

Laser Altimetry of Small-Scale Features on 433 Eros from NEAR-Shoemaker

Andrew F. Cheng,[1]* Olivier Barnouin-Jha,[1] Maria T. Zuber,[2,3] Joseph Veverka,[4] David E. Smith,[3] Gregory A. Neumann,[2] Mark Robinson,[5] Peter Thomas,[4] James B. Garvin,[3] Scott Murchie,[1] Clark Chapman,[6] Louise Prockter[1]

During the Near Earth Asteroid Rendezvous (NEAR)–Shoemaker's low-altitude flyover of asteroid 433 Eros, observations by the NEAR Laser Rangefinder (NLR) have helped to characterize small-scale surface features. On scales from meters to hundreds of meters, the surface has a fractal structure with roughness dominated by blocks, structural features, and walls of small craters. This fractal structure suggests that a single process, possibly impacts, dominates surface morphology on these scales.

The NEAR-Shoemaker mission (*1*) has measured the shape of asteroid 433 Eros from orbit with a laser altimeter (*2*), enabling quantitative assessments of the asteroid's surface morphology at scales of hundreds of meters to kilometers (*3*). Previous results from the NLR (*4*) suggested that Eros is a consolidated object whose shape is dominated by collisions. Clustered steep slopes, beyond expected angles of repose, are present over ~2% of the surface area (*4*). During the low-altitude flyover of Eros on 26 October 2000, simultaneous observations with the NLR and the multispectral imager (MSI) were obtained at a spatial resolution of ~1 m, which is at least three times the resolution achieved previously (*5*).

During the flyover, the NLR was operated continuously at a 2-Hz pulse repetition frequency. The NLR range precision is ~1 m, and the NLR boresight direction, which is illuminated by the laser, is close to the center of the MSI image field of view (*3, 6–8*). As the surface moves past the instrument boresight (owing to orbital motion, asteroid rotation, and spacecraft maneuvers), the laser spots trace out a track

[1]The Johns Hopkins University Applied Physics Laboratory, Laurel, MD 20723–6099, USA. [2]Department of Earth, Atmospheric, and Planetary Sciences, Massachusetts Institute of Technology, Cambridge, MA 02139, USA. [3]Earth Sciences Directorate, NASA/Goddard Space Flight Center, Greenbelt, MD 20771, USA. [4]Space Sciences Building, Cornell University, Ithaca, NY 14853, USA. [5]Department of Geological Sciences, 309 Locy Hall, Northwestern University, Evanston, IL 60208, USA. [6]Southwest Research Institute, 1050 Walnut Street, Suite 426, Boulder, CO 80302, USA.

*To whom correspondence should be addressed. E-mail: andrew.cheng@jhuapl.edu